Behavioral/Cognitive

Cortical Cholinergic Input Is Required for Normal Auditory Perception and Experience-Dependent Plasticity in Adult Ferrets

Nicholas D. Leach, Fernando R. Nodal, Patricia M. Cordery, Andrew J. King, and Victoria M. Bajo
Department of Physiology, Anatomy, and Genetics, University of Oxford, Oxford OX1 3PT, United Kingdom

The nucleus basalis (NB) in the basal forebrain provides most of the cholinergic input to the neocortex and has been implicated in a variety of cognitive functions related to the processing of sensory stimuli. However, the role that cortical acetylcholine release plays in perception remains unclear. Here we show that selective loss of cholinergic NB neurons that project to the cortex reduces the accuracy with which ferrets localize brief sounds and prevents them from adaptively reweighting auditory localization cues in response to chronic occlusion of one ear. Cholinergic input to the cortex was disrupted by making bilateral injections of the immunotoxin ME20.4-SAP into the NB. This produced a substantial loss of both p75 neurotrophin receptor ($p75^{NTR}$)-positive and choline acetyltransferase-positive cells in this region and of acetylcholinesterase-positive fibers throughout the auditory cortex. These animals were significantly impaired in their ability to localize short broadband sounds (40 –500 ms in duration) in the horizontal plane, with larger cholinergic cell lesions producing greater performance impairments. Although they localized longer sounds with normal accuracy, their response times were significantly longer than controls. Ferrets with cholinergic forebrain lesions were also less able to relearn to localize sound after plugging one ear. In contrast to controls, they exhibited little recovery of localization performance after behavioral training. Together, these results show that cortical cholinergic inputs contribute to the perception of sound source location under normal hearing conditions and play a critical role in allowing the auditory system to adapt to changes in the spatial cues available.

Introduction

Cortical release of the neuromodulator acetylcholine (ACh) has been implicated in various cognitive functions, including attention, learning, and memory (Weinberger, 2003; Hasselmo and Sarter, 2011; Klinkenberg et al., 2011; Letzkus et al., 2011; Edeline, 2012). Much of the evidence for this comes from studies showing that the response properties of cortical neurons can be modulated by the activation or blockade of cholinergic inputs in ways that might support these functions (Sillito and Kemp, 1983; Metherate et al., 1992; Oldford and Castro-Alamancos, 2003; Disney et al., 2007; Herrero et al., 2008; Goard and Dan, 2009; Bhattacharyya et al., 2012). In the auditory system, for example, pairing sounds with electrical stimulation of the nucleus basalis (NB), which provides the major source of cortical ACh (Lehmann et al., 1980; Mesulam et al., 1983), induces stimulus-specific representational plasticity both in the cortex (Bakin and Weinberger, 1996; Kilgard and Merzenich, 1998a,b; Bao et al., 2003; Froemke et al., 2007) and at subcortical levels (Ma and Suga, 2003; Zhang and Yan, 2008), that closely resembles the changes observed after sound discrimination learning (Weinberger, 2003).

These findings suggest that ACh release may represent a mechanism by which behavioral meaning becomes bound to sensory stimuli. This is supported by the finding that pairing NB stimulation with tone presentation induces auditory memory (Weinberger et al., 2006) and promotes discrimination learning (Reed et al., 2011) for that tone frequency. However, although cholinergic-dependent plasticity in response to the presentation of pure tone stimuli has been extensively studied, how NB cholinergic inputs affect auditory perception and learning in more complex tasks remains unclear.

The direction of a sound source is computed by the brain using differences in the intensity and timing of sounds arriving at the two ears, together with the spectral cues produced by the way sounds interact with the folds of the external ear (Schnupp et al., 2010). Although these cues are processed subcortically, an intact auditory cortex is vital for accurate sound localization (Jenkins and Masterton, 1982; Heffner and Heffner, 1990; Nodal et al., 2010) and for the ability to learn to overcome temporary perturbations in the composition of auditory spatial cues that result from occlusion of one ear (Bajo et al., 2010; Nodal et al., 2010, 2012).

In this study, we investigated the role of cortical ACh release in the generation of a sound location percept and the ability to recalibrate this percept during perturbed listening conditions.

Received Oct. 27, 2012; revised Feb. 3, 2013; accepted March 8, 2013.

Author contributions: V.M.B., N.D.L., and A.J.K. designed research; N.D.L., V.M.B., F.R.N., A.J.K., and P.M.C. performed research; N.D.L., V.M.B., F.R.N., and P.M.C. analyzed data; N.D.L., V.M.B., F.R.N., and A.J.K. wrote the paper.

This work was supported by Wellcome Principal Research Fellowship WT076508AIA (A.J.K.) and a Deafness Research UK studentship (N.D.L.). We are grateful to R. Campbell, A. Isaiah, P. Keating, D. Kumpik, and S. Spires who contributed to the behavioral testing.

Correspondence should be addressed to Dr. Victoria M. Bajo, Department of Physiology, Anatomy, and Genetics, University of Oxford, Parks Road, Oxford OX1 3PT, UK. E-mail: victoria.bajo@dpag.ox.ac.uk.

DOI:10.1523/JNEUROSCI.5039-12.2013

 0270-6474/13/336659-13$15.00/0

Cholinergic manipulation was achieved by destroying cortically projecting cholinergic neurons using a selective immunotoxin injected directly into the NB of adult ferrets. We found that animals with extensive cortical cholinergic deafferentation caused by the immunotoxin injections were substantially impaired in their ability to accurately localize sounds, particularly at shorter stimulus durations, and exhibited much less adaptation to altered sound localization cues. Therefore, ACh appears to be necessary for the accurate generation of a sound location percept and the mechanism by which this system recalibrates itself according to experience.

Materials and Methods

Fourteen adult pigmented ferrets were used in these experiments, comprising seven animals with bilateral injections of the immunotoxin ME20.4-SAP in the NB and six controls (including two with NB sham injections). One additional control received ME20.4-SAP injections outside the NB (in the caudate nucleus). All experimental procedures were performed following local ethical review committee approval and under license from the United Kingdom Home Office in accordance with the Animal (Scientific Procedures) Act (1986).

Sound localization paradigm. The sound localization paradigm used in this study has been described previously (Kacelnik et al., 2006; Nodal et al., 2008). Briefly, animals were positively conditioned to approach broadband noise stimuli, presented from 1 of 12 speakers situated around the periphery of a circular testing chamber. Animals were motivated to perform the sound localization task by water regulation, their daily water intake comprising water obtained during the task and that supplied after testing.

Sound localization testing took place within a sound-proof chamber lined with 50 mm Melatech sound absorbing foam (The Noise Control Centre). The speakers (50 W dome tweeters, AUDAX TW025M0; Falcon Acoustics) were hidden behind a muslin curtain to prevent use as a visual cue to sound location, and each was positioned over a reward spout.

Gaussian broadband noise (0.5–30 kHz, 5 ms rise/fall time) was generated using Tucker Davis Technologies System II hardware. The sound level was randomized in one-fifth octave bands (level was boosted or attenuated by a random number of decibels drawn from a normal distribution: mean $\pm$ SD, 0 $\pm$ 5 dB) to minimize the possibility of the ferrets learning differences in the output of individual speakers. Stimulus duration (40, 100, 200, 500, 1000, or 2000 ms) and overall level (56–84 dB SPL, in 7 dB intervals) were controlled with custom-written MATLAB software (version 7.0.4; MathWorks). Although stimulus duration was fixed during each testing session, the level was roved pseudorandomly to prevent ferrets using absolute sound level as a cue for sound location.

Behavioral data collection. Ferrets were trained to initiate approach-to-target trials by licking a central spout, ensuring that the head was consistently positioned at the center of the testing chamber before stimulus generation. If a ferret correctly identified the location of the sound by licking the spout beneath the speaker from which the stimulus had been presented, it was rewarded with a fixed amount of water. Potential bias toward particular speaker locations was controlled for with correction and "easy" stimuli, which respectively comprised repetitions of the initial stimulus or continuous noise. Motivation was maintained during testing by rewarding animals from the central spout on 5% of trials. Neither the correction and easy trials nor those trials in which animals received a reward from the central spout were included in the analysis. Typically, animals were tested initially at the longest stimulus duration (2000 ms). Stimulus duration was consecutively shortened after completion of >300 individual trials during each 14 d testing block.

Unconditioned head orienting movements toward auditory stimuli were recorded for the first 1000 ms after stimulus presentation using a reflective strip attached to the head and an overhead infrared camera and video contrast detection device (HVS Image). Custom-written MATLAB software calculated the change in head angle offline, discarding anticipatory or delayed orienting responses (Nodal et al., 2008) and trials in which initial head placement deviated by >10° from the session mean. Traces were smoothed using a moving three-point average. Reaction times were recorded as the latency of the first of the three successive head movements made in the same direction. The initial head turn was considered over when a change in the direction of the movement was recorded. The final head bearing was calculated as the mean angle from the last three frames of this initial movement.

Unilateral conductive hearing loss. Animals were fitted with a foam earplug (E.A.R. Classic) under medetomidine hydrochloride sedation (Domitor, 0.1 mg/kg, i.m.; Pfizer).The plug was secured in place in the left ear with Otoform-K2 silicone impression material (Dreve Otoplastik) and veterinary tissue adhesive. Acoustical measurements indicated that these earplugs produced 40–50 dB of attenuation at frequencies of >3.5 kHz, which rolled off gradually at lower frequencies.

Cholinergic immunotoxin. ME20.4-SAP (Advanced Targeting Systems) comprises a monoclonal antibody specific for the p75 neurotrophin receptor ($p75^{NTR}$), a membrane-bound receptor, conjugated to the ribosome-inactivating enzyme saporin. Once ME20.4-SAP is bound to the external cell membranes, the saporin toxin is internalized and prevents protein synthesis, resulting in neuronal cell death (Pizzo et al., 1999). This receptor is expressed primarily by cholinergic neurons in the basal forebrain (Kordower et al., 1989; Tremere et al., 2000).

Surgery. All surgical procedures were performed under isoflurane anesthesia. Briefly, anesthesia was induced with Domitor (0.022 mg/kg, i.m.) and ketamine (Ketaset, 5 mg/kg, i.m.; Fort Dodge Animal Health) and subsequently maintained with isoflurane (IsoFlo; 0.5–2.5%; Abbott Laboratories) in oxygen (1–1.5 L/min) delivered through a closed-loop ventilation system (Harvard Apparatus). Saline was continuously infused (5.0 ml/h) via the radial vein. Body temperature was monitored via a rectal probe and maintained at ~38°C with a Bair Hugger temperature management system (Arizant UK). Respiratory rate, ECG, and end-tidal CO_2 were monitored throughout.

Once stabilized, animals received atipamezole (Antisedan, 0.5 mg/kg, s.c.; Pfizer) to reverse medetomidine sedation. Intraoperatively, animals received methylprednisolone (20 mg/kg, s.c.), buprenorphine (Vetergesic, 0.03 mg/kg, s.c.; Alstoe Animal Health), and meloxicam (Metacam, 0.2 mg/kg, s.c.; Labiana Life Sciences) for analgesia and to prevent inflammation, and cimetidine (Tagamet, 10 mg/kg, i.v.; GlaxoSmithKline) to suppress stomach acid secretions. Atropine sulfate (0.06 mg/kg; AnimalCare) was administered to reduce bronchial secretions. The eyes were protected with Viscotears gel (Novartis).

Pressure injections of ME20.4-SAP or artificial CSF (ACSF) (Harvard Apparatus) in the NB were performed using a glass micropipette, with an internal diameter of 15–20 μm, loaded onto a microinjector (Nanoject II; Drummond Scientific) and attached to a stereotaxic microdrive. Injection coordinates were calculated relative to the bifurcation of the anterior and lateral sulci. Injections were performed in female animals, ~800 g in weight, to minimize differences in brain anatomy and reduce the likelihood of misplaced injections. In one animal, the coordinates were changed to allow ME20.4-SAP to be injected into the caudate nucleus, which contains cholinergic neurons that do not express $p75^{NTR}$.

Micropipettes were prefilled with silicone oil followed by either ME20.4-SAP (0.32 mg/ml) in ACSF or ACSF alone. Four injections in the same coronal plane were made in each hemisphere, along two injection tracks separated laterally by 200 μm and at two depths separated by an additional 200 μm. Each injection comprised a total volume of 27.6 nl, and 35.2 ng of ME20.4-SAP was delivered to each hemisphere in total. Pipettes were left *in situ* for 5 min after each pressure injection to prevent the flow of immunotoxin or ACSF back along the injection track.

Postoperatively, all animals received buprenorphine (0.03 mg/kg, s.c.), methylprednisolone (10 mg/kg, s.c.), and Metacam (0.05 ml, p.o.) and were allowed at least 1 week to recover from surgery before subsequent behavioral testing.

Histology. Animals were sedated with Domitor and overdosed with Euthatal (2 ml of 200 mg/ml pentobarbital sodium; Merial Animal Health), before transcardial perfusion with ~300 ml of 0.9% saline, followed by 1 L of 4% paraformaldehyde in 0.1 M phosphate buffer (PB), pH 7.4. After removal from the skull, brains were cryoprotected by immersion in 30% sucrose in 0.1 M PB for several days. Brains were sectioned in the coronal plane, anterior to posterior, using a Leica SM200R microtome.

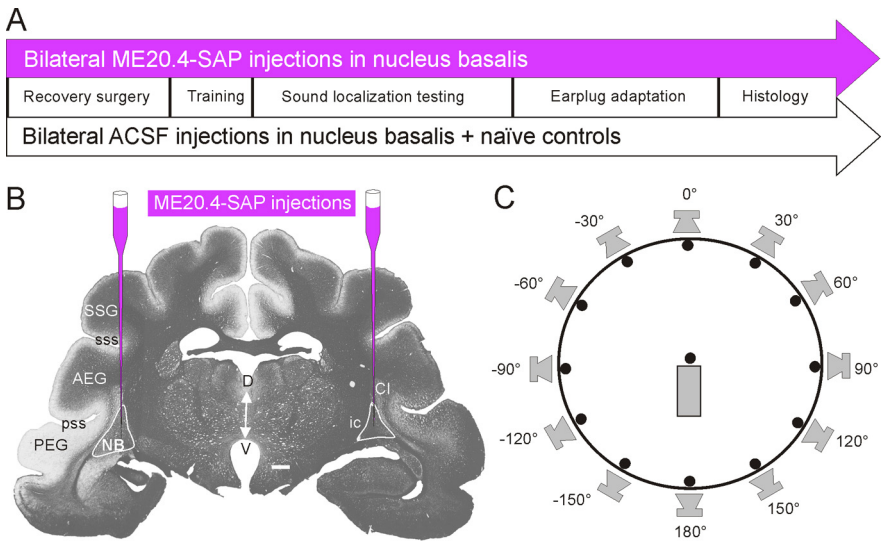

Figure 1. Overview of experimental procedures. ***A***, Time lines for the two main experimental groups used in this study. Injections of ME20.4-SAP or ACSF in the NB were performed before behavioral training. Subsequently, animals were tested for their ability to localize sounds in azimuth both under normal hearing conditions and then in the presence of a unilateral earplug, before perfusion and histology. ***B***, Photograph of a coronal section of a ferret brain, stained for myelin using the Gallyas method, at the level of the auditory cortex and the NB, illustrating the position of ME20.4-SAP immunotoxin injections. ***C***, Ferrets were trained by positive conditioning to approach the perceived location of an auditory stimulus presented from 1 of 12 speakers arranged around the periphery of a circular chamber. Animals initiated trials by standing on a central platform and licking the associated spout for at least 300 ms. Scale bar (in ***B***), 1 mm. AEG, Anterior ectosylvian gyrus; CI, claustrum; D, dorsal; ic, internal capsule; PEG, posterior ectosylvian gyrus; pss, pseudosylvian sulcus; SSG, suprasylvian gyrus; sss, suprasylvian sulcus; V, ventral.

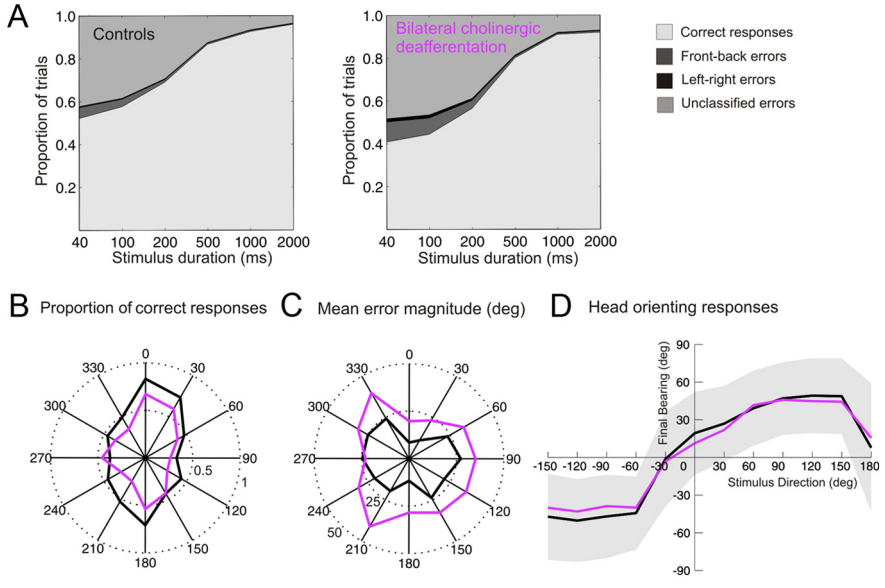

Figure 2. Effect of cortical ACh depletion on auditory localization performance. ***A***, Approach-to-target localization responses at each stimulus duration. Correct responses are shown in light gray, and incorrect responses are further subdivided into front–back errors (dark gray), left–right errors (black), and unclassified errors (mid-gray). ***B***, Polar plot illustrating the proportion of correct responses (radial axis) at each peripheral speaker position for the two experimental groups when tested with 40 ms duration stimuli. Control animals are shown in black and animals with ME20.4-SAP cholinergic lesions in purple. ***C***, Polar plot showing the mean error magnitude (radial axis, degrees) for each speaker position for a stimulus duration of 40 ms. ***D***, Head orienting responses obtained in the same trials. Mean final head bearing is plotted against stimulus direction for each experimental group. The shaded region represents 1 SD about the mean for the control animals. The broadly sigmoidal dependence of head bearing on stimulus location was conserved across the two experimental groups.

On the sections, the Nissl substance was stained with 0.5% cresyl violet, the myelin by the Gallyas method (Gallyas, 1979), and putative cortical cholinergic fibers were visualized with acetylcholinesterase (AChE) histochemistry (Tago et al., 1986; Kamke et al., 2005a). Antibodies against non-phosphorylated (H) neurofilaments (1:1000, anti-SMI_{32} mouse monoclonal antibody; Covance Research Products) and neuron-specific nuclear protein (1:1000, catalog #MAB377, anti-NeuN mouse monoclonal antibody; Millipore) were used to label neurofilaments (SMI_{32}) and neurons (NeuN), respectively. Choline acetyltransferase (ChAT) (1:1000, catalog #AB143, rabbit polyclonal antibody; Millipore) and $p75^{NTR}$ (1:500, catalog #AB-N07, anti-$p75^{NTR}$ mouse monoclonal antibody, ME20.4; Advanced Targeting Systems) immunoreactivity was used to provide two markers of cholinergic neurons (Tremere et al., 2000), and parvalbumin (PV) (1:6000, anti-PV mouse monoclonal antibody; Sigma-Aldrich) expression was used to identify putative GABAergic cortical projecting neurons in the basal forebrain (Gritti et al., 2003).

Sections were incubated in the corresponding primary antibodies after reducing nonspecific binding by preincubation in 5% normal horse serum in PB saline and then incubated for 2 h in the secondary antibody (biotinylated horse anti-rabbit or anti-mouse IgG; 1:200 dilution; Vector Laboratories), followed by 90 min in avidin biotinylated enzyme complex (ABC; Vector Laboratories), before visualization using 3,3'-diaminobenzidine. Sections were mounted on gel-coated slides, dried, dehydrated with absolute ethanol, cleared with xylene, and coverslipped with DePex mounting media. Positive and negative control reactions were performed in parallel for all immunoreactions. Sections from previous experimental animals confirmed positive immunostaining for each protocol, whereas some sections incubated in parallel without primary antibody acted as negative controls.

In an initial set of animals, comprising three controls and three with ME20.4-SAP injections in the NB, the brains were sectioned at 45 μm, and one in every five series of sections was used to stain for Nissl substance, NeuN, AChE, ChAT, and $p75^{NTR}$. In the remaining cases, the brains were cut at 35 μm intervals, and eight sets of sections were collected so that staining for myelin, SMI_{32}, and PV could also be performed. Analysis and quantification of cells, fibers, and terminals were performed using brightfield, optical microscopy. NeuroLucida and StereoInvestigator software (MBF Bioscience, MicroBrightField) were used for histological reconstructions and stereological estimations.

Both ChAT and $p75^{NTR}$ are markers of cholinergic neurons (Tremere et al., 2000), and we have found that ChAT and $p75^{NTR}$ immunoreactive (IR)-positive cells in the ferret NB share a common distribution, morphology, and numbers (Cordery et al., 2009). Although we observed a similar loss of ChAT- and $p75^{NTR}$-IR cells in the animals with ME20.4-SAP injections in the NB, we performed a full quantification on $p75^{NTR}$-IR cells only to avoid erroneously counting ChAT-IR neurons in the neighboring striatum. In addition, the use of a monoclonal antibody against $p75^{NTR}$ gave greater specificity and better labeling of individual cells than the polyclonal antibody available for ChAT.

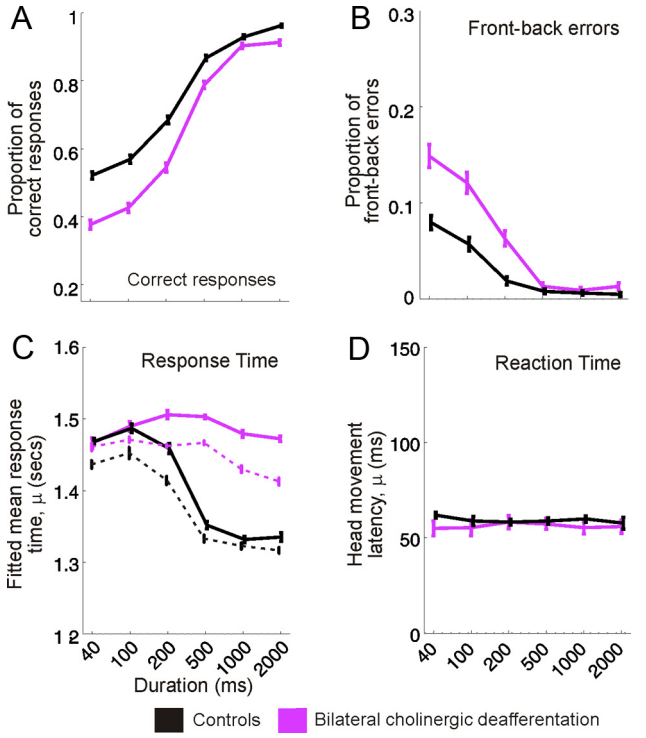

Figure 3. Stimulus duration-dependent effects of cholinergic modulation on localization performance. ***A***, ***B***, Mean ± SD proportion of correct responses and front– back errors, respectively, across stimulus duration for control animals (black) and animals with bilateral cholinergic deafferentation (purple). ***C***, Response time between stimulus onset and the animal licking a peripheral reward spout, fitted using an ex-Gaussian distribution and bootstrapped 100 times, shown relative to stimulus duration for each experimental group. Solid lines represent the response times across all trials and dashed lines for correct trials only. The parameter μ represents the mean ± SD of the normally distributed response times. ***D***, Latency of the initial head movement after sound onset (reaction time) for each experimental group across stimulus duration. The distribution of these reaction times was also described with a high degree of accuracy using an ex-Gaussian distribution, and the value plotted, μ, represents the mean ± SD of the normally distributed head movement latencies.

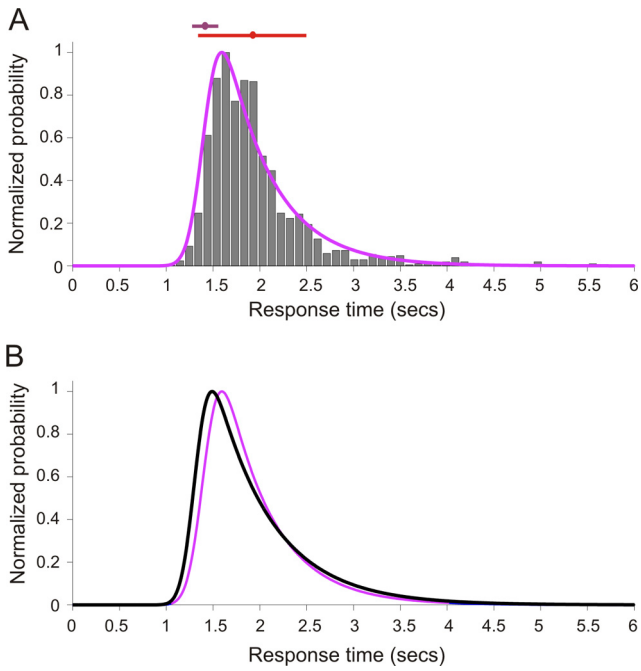

Figure 4. ***A***, Normalized histogram of response times in the approach-to-target localization task for ferrets with immunotoxin lesions of the NB. These values, which are binned at 100 ms, indicate the time between initiating a trial and licking a peripheral reward spout. An ex-Gaussian distribution was used to model these data in MATLAB using the DISTRIB toolbox available from http://darwin.psy.ulaval.ca/~yves/distrib.html. The purple line represents the best-fit, ex-Gaussian model. The mean (μ) and SD (σ) of the Gaussian component of this function are represented by the purple circle and bounding lines, respectively. Mean response time (red circle) and SD (red line) further illustrate the non-normality of this distribution. ***B***, Ex-Gaussian best fit of response times measured for a stimulus duration of 2000 ms in the approach-to-target localization task for ferrets with immunotoxin lesions of the NB (purple) and control animals (black), highlighting the delayed peripheral response times for lesioned ferrets at this stimulus duration.

The number of p75^{NTR}-IR cells (N) was estimated using the fractionator principle according to Konigsmark et al. (1969) by counting the number of positive cells (n) and adjusting this estimation by taking into account the sampling rate (s), section thickness (t), and cell size (r, the minimum mean diameter and m, the minimum diameter measured in the smallest cell in the sample):

$$N = n\left(\frac{s \times t}{t + 2\sqrt{r^2 - m^2}}\right).$$

The density of AChE-positive fibers in the auditory cortex was analyzed in half of the animals (three cases of each group) in which SMI_{32} immunostaining was also available, so that the different regions of the auditory cortex in the ectosylvian gyrus could be distinguished (Bajo et al., 2007). We used the optical fractionator (OF) as a stereological probe by scanning every second or third section using a square grid, 0.09 mm^2, oriented randomly, with a square counting frame of 400 μm^2. Approximately 140 frames were counted within each section, enabling us to determine a coefficient of error and compare population sizes with 95% confidence intervals (Gundersen et al., 1988).

Data analyses. Behavioral data were analyzed using MATLAB, whereas statistical comparisons were performed using the R software package (www.r-project.org). Approach-to-target responses were considered to be independent events after a binomial distribution. Linear mixed effects (lme) models including random effects were used to fit these data, using a binomial family and probit link, to account for random variability between animals. When using statistical tests that assume a Gaussian distribution of data, such as ANOVA, approach-to-target responses were transformed using the following arcsine correction:

$$y = \sin^{-1} \times \sqrt{\frac{x}{n}},$$

where x is the number of, for example, correct responses from the total number, n, of individual trials.

The mutual information (MI) between the approach-to-target stimulus location and final head bearing was calculated as follows:

$$\mathrm{MI}(r; s) = \sum_{r,s} p(r, s) \times \log_2\left(\frac{p(r, s)}{p(r) \cdot p(s)}\right),$$

where r is the final head bearing, s is the stimulus location, $p(r, s)$ represents the joint probability of r and s occurring, and $MI(r; s)$ is the mutual information between r and s. The bias arising from the limited number of head orienting responses analyzed was estimated according to the method proposed by Panzeri et al. (2007) and subtracted from the MI values.

The non-normal distributions of approach-to-target response times and head orienting reaction times were fitted with an ex-Gaussian function using the DISTRIB MATLAB toolbox (http://darwin.psy.ulaval.ca/~yves/distrib.html). Multiple fits were generated ($n = 100$) and statistical tests performed on the bootstrapped fit parameters (μ, τ, and σ) of the ex-Gaussian distribution.

Statistical quantification of changes in sound localization after unilateral ear occlusion was achieved by determining best linear fits for the stimulus–response relationship. To investigate any left-right bias created by the earplug, we transformed the stimulus–response confusion matri-

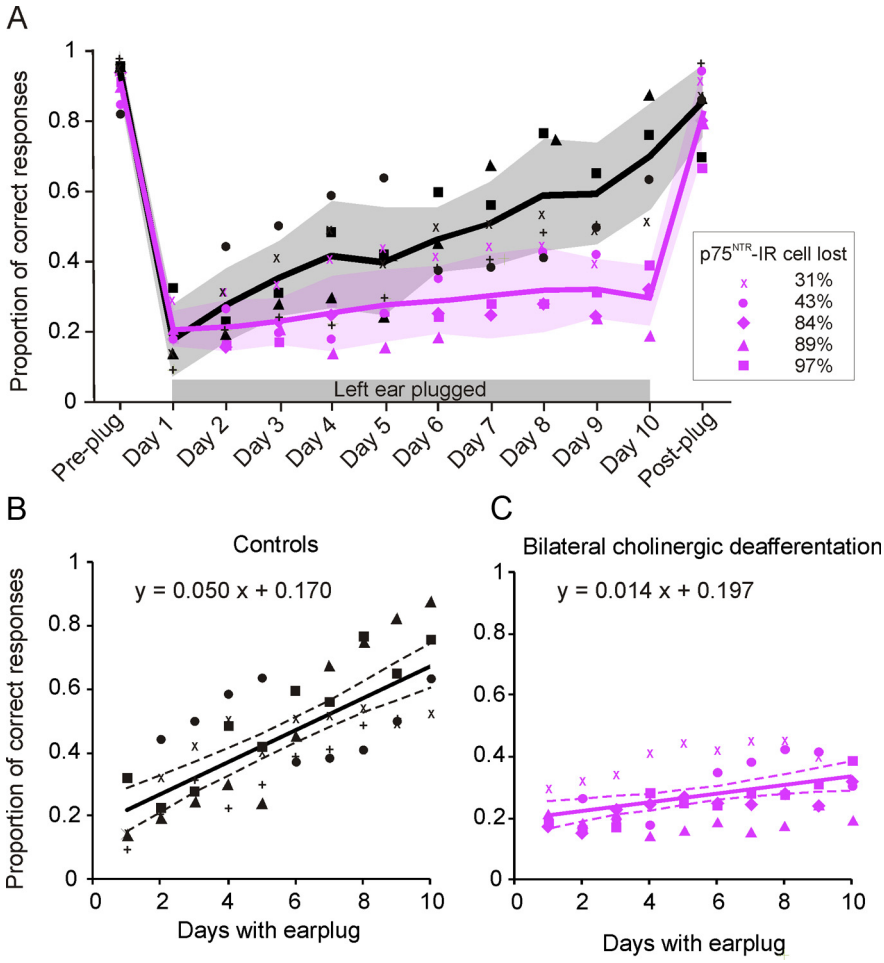

Figure 5. Effect of cortical ACh depletion on behavioral adaptation to a unilateral earplug. ***A***, The proportion of correct responses, averaged over all speaker positions, is plotted for individual animals before earplug insertion (Pre-plug), during training with the earplug in place (Days 1–10), and after earplug removal (Post-plug). Each animal is represented by a different symbol. The mean values for each experimental group are indicated by the solid lines, and the shaded regions show 1 SD about the mean. ***B***, ***C***, Scatter plots showing the calculated linear regressions between the proportion of correct responses and day of wearing an earplug to model the rate of adaptation (slope) to an earplug for the controls (***B***) and animals with bilateral cholinergic lesions (***C***). Symbols represent the data from individual animals, solid lines are the best linear fits, and dashed lines show the 95% confidence intervals of these fits.

ces by folding the anterior and posterior regions on top of each other, thereby removing front-back errors and reducing the approach-to-target response to a lateralization response.

Because of the asymptotic nature of the relationship between head orienting responses and stimulus location, we quantified the effect of cholinergic deafferentation and monaural occlusion on these responses by modeling the orienting errors (stimulus location minus final head bearing) using a quadratic polynomial function. This function was calculated using a robust least-squares method with MATLAB software.

Results

Cortical cholinergic loss impairs sound localization

Normal sound localization data were obtained from all 14 animals used in the study, seven of which received bilateral cholinergic lesions of the NB whereas one received immunotoxin injections in the caudate nucleus, by presenting broadband noise bursts from peripheral speakers located at 30° intervals around the edge of a circular testing chamber (Fig. 1). Two of the animals with immunotoxin NB lesions had to be excluded from the earplug adaptation analysis because of the small number of trials performed; consequently, one of the six control animal was randomly chosen and excluded to equalize the size of the two groups.

Stimulus duration had a large effect on ferret azimuthal localization ability and accounted for >87% of the variance in the responses (ANOVA, $\eta^2 = 0.8740$) (Fig. 2), confirming previous reports from this species (Nodal et al., 2008). The proportion of correct responses decreased at shorter stimulus durations, and there was an increase in overall error magnitude and the proportion of front–back confusions, errors in which an animal localizes a sound to the correct side of the midline but the incorrect side of the interaural axis. Sound localization in control animals that received bilateral injections of ACSF in the NB was indistinguishable from that of naïve controls that had not undergone surgery. Consequently, data collected from animals with bilateral ACSF injections and naïve controls were merged for the subsequent analysis.

Modeling the proportion of correct responses linearly across stimulus location revealed that, relative to controls, animals with cholinergic lesions of the NB were significantly impaired in their ability to localize stimuli shorter than 1000 ms (40–500 ms, $F_{(1,19)} = 21.67, p < 0.001$) but not longer stimuli (1000–2000 ms, $F_{(1,19)} = 3.81, p = 0.066$) (Figs. 2*A*, 3*A*). Decreased performance correlated with an increase in mean error magnitude for the same stimulus durations (40–500 ms, $F_{(1,19)} = 27.21, p < 0.001$; 1000–2000 ms, $F_{(1,19)} = 1.97, p = 0.177$), whereas increases in the incidence of front–back errors were restricted to the three shortest stimulus durations (40–200 ms, $F_{(1,19)} = 16.67, p < 0.001$) (Figs. 2*A*, 3*B*).

To test whether animals with bilateral cholinergic lesions were impaired globally, or only at certain locations, performance was compared in different regions of space. Linear modeling of approach-to-target responses at the four shortest stimulus durations revealed no difference in performance between either the anterior and posterior hemifield (lme interaction, proportion of correct responses, $F_{(1,175)} = 0.063, p = 0.802$; mean unsigned error, $F_{(1,175)} = 0.311, p = 0.528$) or the left and right hemifield (lme interaction, proportion of correct responses, $F_{(1,175)} = 0.597, p = 0.441$; mean unsigned error, $F_{(1,175)} = 1.16, p = 0.284$). Thus, bilateral cholinergic deafferentation resulted in less accurate localization of short-duration sounds throughout the horizontal plane (Fig. 2*B*,*C*).

The time between the animal triggering the presentation of a stimulus, by licking the start spout at the center of the arena, and making its response by licking one of the 12 peripheral reward spouts was also modified by immunotoxin injections in the NB. As in previous studies of response times (Lacouture and Cousineau, 2008), we fitted these data using an ex-Gaussian distribution (Fig. 4*A*), which revealed a clear difference in the mean of the Gaussian region (μ) of the response time distribution between

animals with bilateral cholinergic deafferentation and controls (Figs. 3*C*, 4*B*). Stimulus duration had a significant effect on the linearly modeled μ parameter when the experimental groups were examined in parallel (lme, $F_{(1,126)} = 24.151$, $p < 0.001$) and a significant condition–duration interaction term confirmed that response times for animals with bilateral cholinergic deafferentation were significantly increased at longer stimulus durations (lme, $F_{(1,126)} = 4.170$, $p < 0.05$) (Fig. 3*C*). Consistent with previous measurements of response times in ferrets (Nodal et al., 2008), we found that these values were shorter in both groups when the animals made a correct response than when they mislocalized the sound source. The difference between the groups was not attributable exclusively to abnormally long response times on incorrect trials, because the animals with cholinergic lesions also took longer than the controls to select a reward spout when a correct decision was made (Fig. 3*C*). Thus, although localization accuracy at longer stimulus durations was unaffected by cholinergic lesions of the NB, the animals took significantly longer to make these responses.

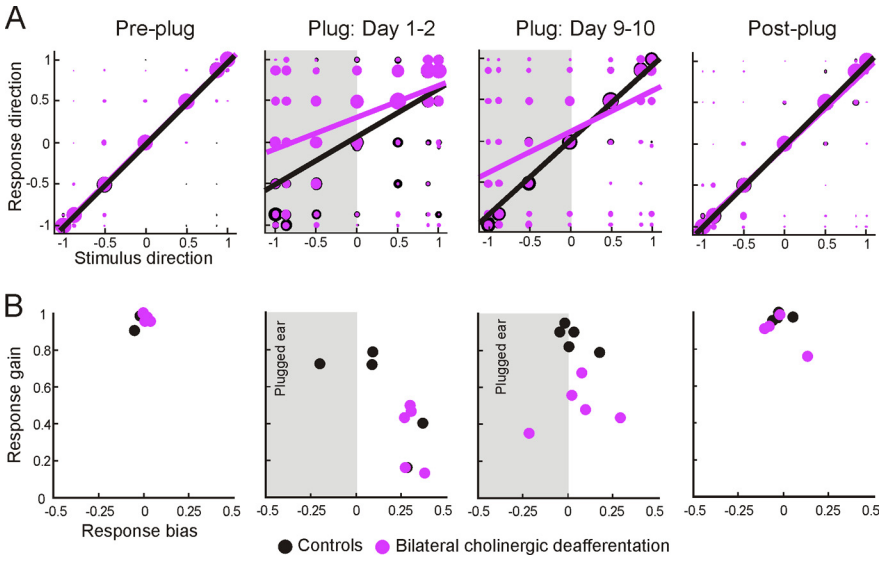

Figure 6. Changes in response bias and gain during adaptation to a unilateral earplug. ***A***, Confusion matrices of approach-to-target responses for animals with bilateral cholinergic deafferentation and controls. Stimulus and response locations have been transformed in azimuthal space so that the posterior and anterior portions of the circular response space are "folded" onto each other, effectively turning all errors into lateral errors. Regression lines indicate the best linear fit of the stimulus–response function before plug insertion (Pre-plug), at two time points during training with the earplug in place (Plug: Day 1–2, Plug: Day 9–10), and after plug removal (Post-plug), for animals with bilateral cholinergic lesions (purple) and controls (black). Perfect performance equates to a slope of one and a *y*-intercept of zero. Deviations from these values indicate impaired localization performance. Note that the responses become biased toward the non-occluded ear when the earplug is first inserted. ***B***, Plots illustrating changes in response bias (*y*-intercept) and response gain (slope), calculated from the stimulus–response linear regressions, for individual animals in both groups. Shaded areas indicate where the left ear was plugged.

In addition to measuring categorized approach-to-target localization responses, unconditioned head orienting responses, captured using a reflective head strip, were used to provide an absolute measure of sound localization ability and generate reaction time data. Stimulus direction accounted for >95% of the variance in these orienting responses (ANOVA, $\eta^2 = 0.966$), and bilateral cholinergic deafferentation explained none (ANOVA, $\eta^2 = 0$) (Fig. 2*D*). To quantify the accuracy of these responses, we estimated the amount of information the final head bearing conveyed about the direction of the target sound. Although there was a small, but significant, reduction in the mutual information between final head bearing and target location at shorter stimulus durations for control and lesioned groups (lme, $F_{(1,37)} = 4.9409$, $p < 0.05$), reflecting concomitant changes in approach-to-target performance, there was no interaction between cholinergic impairment and stimulus duration (lme, $F_{(1,37)} = 0.004$, $p = 0.949$). This suggests that the impairments observed when the animals with bilateral cholinergic lesions had to select which target location to approach to receive a reward cannot be accounted for by changes in head orienting accuracy.

Furthermore, reaction times, defined as the latency between stimulus onset and the initiation of a head orienting movement, were unchanged by cholinergic lesions. Mean ± SD reaction times for control animals and those with bilateral cholinergic lesions were 154.7 ± 89.2 and 151.2 ± 100.8 ms, respectively. Modeling these data using an ex-Gaussian distribution, as shown for the response times in Figure 4, and fitting linearly across stimulus duration confirmed that bilateral cholinergic deafferentation did not significantly affect either the mean of the Gaussian region of the reaction time distribution, μ (lme, $F_{(1,12)} = 0.0726$, $p = 0.792$) or the parameter associated with the skewed tail, τ (lme, $F_{(1,12)} = 0.2015$, $p = 0.662$), which represents longer-latency orienting responses (Figs. 3*D*, 4).

Therefore, these data show that auditory localization performance was impaired after loss of cortical cholinergic inputs originating in the NB and that this impairment was apparent only when the animals had to approach the perceived location of the sound source.

Reduced ability to adapt to altered localization cues

The influence of cortical ACh release on auditory perceptual plasticity was investigated by testing whether the ferrets were able to recover their ability to localize sound after occluding one ear with an earplug. Monaural occlusion initially disrupts localization accuracy, but when provided with appropriate behavioral training, both ferrets (Kacelnik et al., 2006) and humans (Kumpik et al., 2010) rapidly learn to localize accurately again. We found that the control animals exhibited normal learning, whereas ferrets with bilateral cholinergic lesions were substantially impaired in their ability to adapt to altered spatial cues.

The effect of loss of cholinergic function on the rate of adaptation to the earplug was investigated by modeling performance linearly over a 9–10 d training period (Fig. 5*A*). Multiple between-group comparisons of the proportion of correct responses across speaker location over the training period revealed a significantly reduced rate of adaptation for animals with bilateral cholinergic deafferentation relative to controls (ANCOVA, $F_{(1,97)} = 53.41$, $p < 0.01$) (Fig. 5*A–C*). The slopes of the linear regressions fitted to the percentage correct scores from each group were significantly different (ANOVA, $F_{(1,94)} = 23.47$, $p < 0.01$), confirming that the rate of adaptation in lesioned animals was reduced despite the overall variability in performance observed between individual animals (Fig. 5*B*,*C*). Testing the effect of response hemifield on the rate of adaptation revealed significant interactions on both the left and right sides of space (left, $t_{(1,77)} = 7.940$, $p = 0.006$; right, $t_{(77)} = 37.905$, $p < 0.001$), indicating that adaptation rate in both hemifields was affected by cholinergic deafferentation.

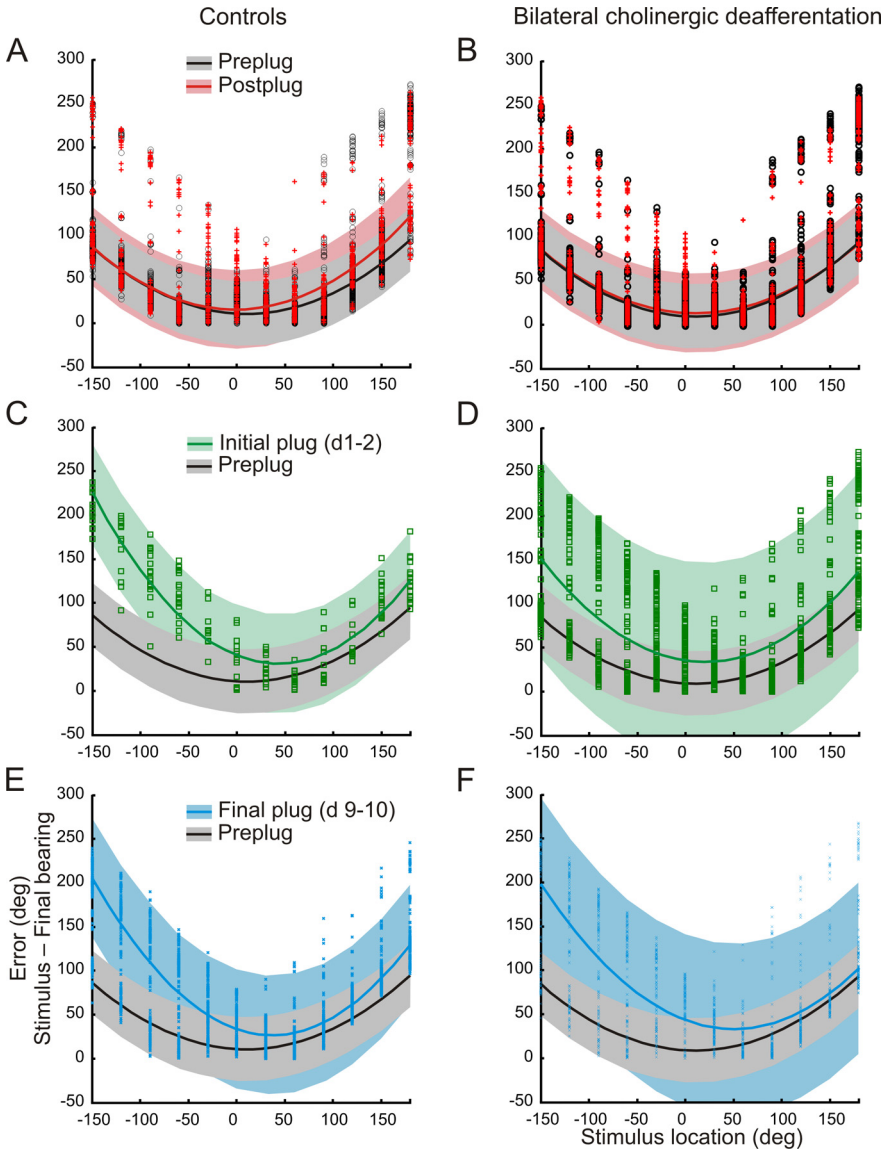

Figure 7. Effects of a unilateral earplug on the sound-evoked head orienting errors (stimulus location minus final head bearing) made by control ferrets (left column) and animals with bilateral cholinergic lesions of the NB (right column). Each panel shows data from individual trials together with the fitted quadratic polynomial curves calculated using a robust least-squares method (bisquare weights). Shaded regions indicate the 95% confidence intervals in each case. ***A***, ***B***, Distribution of the errors before insertion of the earplug (Pre-plug) and after its removal (Post-plug) for both groups. ***C***, ***D***, Head orienting errors made during the first 2 d of wearing an earplug (Initial plug). The pre-plug curve fit and 95% confidence intervals are also shown for comparison. Note the greater variability in the size of the errors in the animals with cholinergic lesions (***D***) than in the controls (***C***). ***E***, ***F***, Head orienting errors made during the last 2 d (9 and10) of wearing an earplug. The pre-plug curve fit and 95% confidence intervals are again shown for comparison.

To further quantify the effect of occluding one ear on localization accuracy and its recovery with training, we measured the gain and bias in the relationship between stimulus and approach-to-target response location. This takes into account the distribution of all the responses made by the animals rather than just the proportion of correct scores. Figure 6 shows linear least-squares fits to the data, which have been transformed to remove the effect of front–back errors so as to emphasize bias to the left or right sides of space. For both groups, plugging one ear resulted in a reduction in the slope (response gain) of these linear fits and the intercept shifted, indicating a response bias toward the non-occluded ear. Both the gain and the bias subsequently showed some recovery during the training period, but this recovery was much more complete for control animals. This is illustrated both by a difference in the response gain between the groups (lme, $F_{(1,32)} = 15.39$, $p < 0.001$) and confirmed by within-group analyses, which revealed a significant increase in gain with training in the control animals ($F_{(1,8)} = 6.39$, $p = 0.035$) but not in the cholinergic deafferented ferrets ($F_{(1,8)} = 2.79$, $p = 0.130$).

In the first session after earplug removal, the performance of the ferrets in both groups returned to very close to their pre-plug values (Figs. 5, 6). This lack of any appreciable aftereffect is consistent with previous studies (Kacelnik et al., 2006; Kumpik et al., 2010).

The effect of monaural occlusion on the head orienting responses was also examined. Because of the asymptotic relationship between final head bearing and stimulus location (Fig. 2*D*), we calculated the orienting errors and modeled them using a quadratic polynomial function calculated using a robust least-squares method (bisquare weights). This model produced a good fit ($R^2 \geq 0.8$) to the responses made before insertion of the earplug and after its removal for both experimental groups (Fig. 7*A*,*B*).

In the control animals, monaural occlusion initially resulted in larger head orienting errors, particularly for stimulus locations within the hemifield ipsilateral to the occluded (left) ear (Fig. 7*C*) (pre-plug errors: left hemifield, 56.8 ± 45.7°; right hemifield, 52.1 ± 44.6°; initial plug errors: left hemifield, 136.9 ± 51.1°; right hemifield, 51.1 ± 51.9°). By the end of the 10 d training period, a partial recovery in the accuracy of the head orienting responses had occurred (left hemifield errors, 107.8 ± 65.4°; right hemifield errors, 49.4 ± 37.7°), as indicated by the greater overlap with the pre-plug data (Fig. 7*E*). This is consistent with previous reports showing that the initial head orienting responses partially adapt with training to the presence of a unilateral hearing loss (Kacelnik et al., 2006; Nodal et al., 2010).

Monaural occlusion also disrupted the head orienting responses made by the ferrets with cholinergic NB lesions (Fig. 7*D*) (pre-plug errors: left hemifield, 50.5 ± 41.6°; right hemifield, 41.4 ± 46.1°; initial plug errors: left hemifield, 95.1 ± 65.7°; right hemifield, 51.1 ± 51.9°). More importantly, the range of errors made when the earplug was first inserted was much greater in these animals (Fig. 7*D*) and the model provided a much worse fit to the data ($R^2 = 0.30$) than in the control group ($R^2 = 0.79$). Thus, altering auditory spatial cues resulted in considerably more variable orienting responses in the animals with cholinergic lesions, as indicated by the much larger confidence intervals, rather than just biasing them toward the side of the open ear. Sound

localization training during the period of monaural occlusion had little effect on the variability of these responses, and, in contrast to the control group, no reduction in error size was observed for stimulus locations ipsilateral to the occluded ear (Fig. 7*F*) (final plug errors: left hemifield, 116.9 ± 70.6°; right hemifield, 45.1 ± 43.7°).

Closer examination of the head orienting errors in the right hemifield (the side of the open ear) revealed no differences across the four time points (before earplug insertion, the initial 2 d and final 2 d of wearing the plug, and after plug removal) shown in Figure 7 ($F_{(3,4463)} = 1.639$, $p = 0.178$) and no interaction between group and time point. However, in the left hemifield (the side of the earplug), we found significant differences in error magnitude both between controls and lesioned animals ($F_{(1,4505)} = 27.66$, $p < 0.0001$) and across the different time points ($F_{(3,4505)} = 292.97$, $p < 0.0001$), as well as a significant interaction between them ($F_{(3,4505)} = 15.59$, $p < 0.0001$). This confirms that head orienting accuracy was impaired primarily on the side of the occluded ear and that this shows less recovery with training in the ferrets with cholinergic lesions. Therefore, these findings are consistent with the approach-to-target data in showing that cholinergic deafferentation impairs adaptation to altered auditory spatial cues.

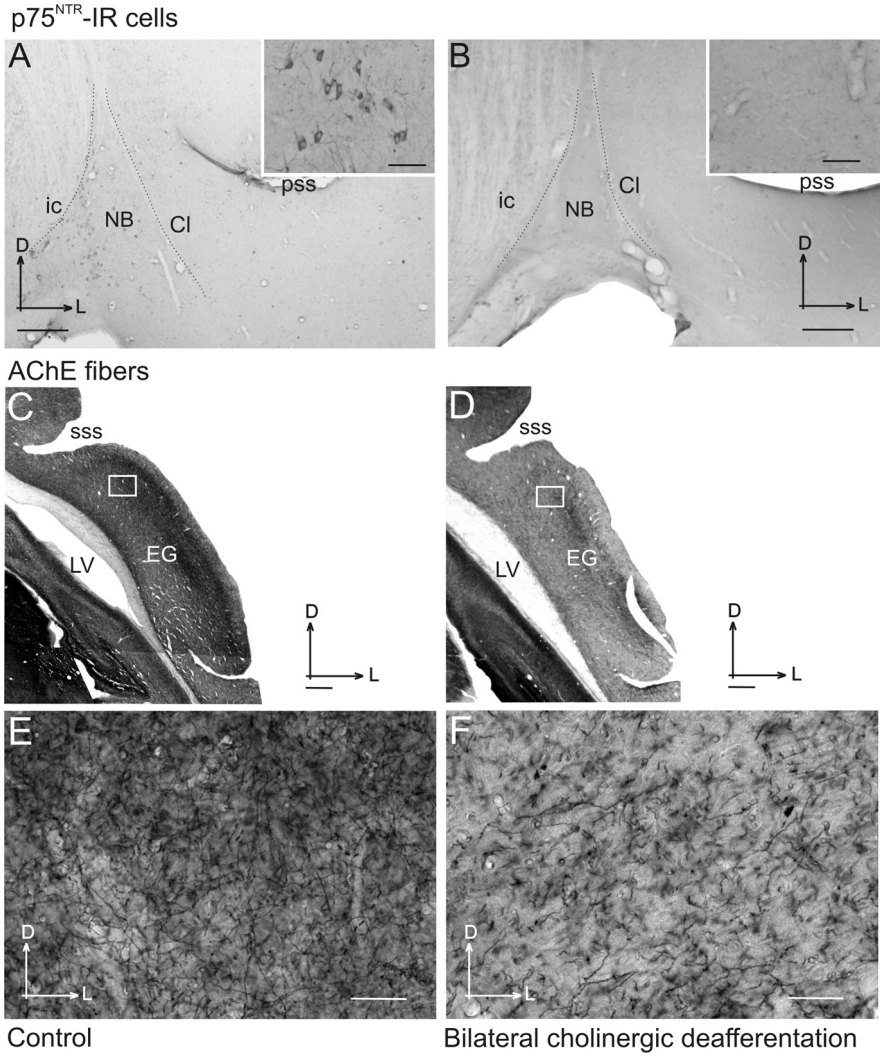

Figure 8. Cholinergic inputs from the NB to the auditory cortex. ***A***, ***B***, Coronal sections taken at the level of the NB immunostained to visualize p75 ^{NTR} cells in a control animal (***A***) and an animal in which bilateral ME20.4-SAP injections had been made in the NB (***B***). Insets show a higher-magnification view of the most medial region of the NB, in which the cells are most densely packed. ***C***, ***D***, Photographs taken at low magnification from coronal sections in the same animals stained to visualize AChE fibers in the ectosylvian gyrus, in which the auditory cortex is located. The regions indicated by the white rectangles in each of these panels are shown at higher magnification in ***E*** and ***F***, respectively, and illustrate the density of AChE fibers within the supragranular layers of the auditory cortex. All four pictures were taken with exactly the same light and filter conditions at the microscope, and no additional computer manipulations of contrast or brightness were performed. Scale bars: ***A***, ***B***, 200 μm; insets, 50 μm; ***C***, ***D***, 1 mm; ***E***, ***F***, 100 μm. Cl, Claustrum; D, dorsal; EG, ectosylvian gyrus; ic, internal capsule; L, lateral; LV, lateral ventricle; pss, pseudosylvian sulcus; sss, suprasylvian sulcus.

Quantifying reduced cholinergic function in the cortex

The number of cholinergic neurons in the NB and the density of cholinergic fibers in the auditory cortex were determined histologically (Fig. 8, Table 1). Relative to controls (Fig. 8*A*), we observed a significant decrease in the number of p75 ^{NTR}-IR neurons in the NB of the ferrets with bilateral ME20.4-SAP injections (Fig. 8*B*) (*t* test, $t_{(5.6)} = 7.03$, $p < 0.001$). Neither the number of PV-IR cells in the NB (*t* test, $t_{(8)} = 2.06$, $p = 0.07$) nor the number of p75 ^{NTR}-IR neurons in the medial septum (*t* test, $t_{(5)} = 0.57$, $p = 0.59$) (Figs. 9, 10, Table 1) were altered by our experimental manipulation, confirming that cell loss was specific for p75 ^{NTR}-IR neurons in the NB of animals that received immunotoxin lesions.

The density of AChE fibers throughout the ectosylvian gyrus was similarly reduced in animals with bilateral ME20.4-SAP injections (Fig. 8*D*,*F*) relative to controls (Fig. 8*C*,*E*) (ANOVA, $F_{(1,45)} = 5.072$, $p = 0.029$). We observed a significant effect of cortical region (medial, anterior, or posterior ectosylvian gyrus) on AChE fiber density (ANOVA, $F_{(2,45)} = 3.233$, $p = 0.049$), indicating regional differences across the auditory cortex in the density of cholinergic innervation (Table 1). However, the lack of an interaction between experimental group and cortical region (ANOVA, $F_{(2,45)} = 0.007$, $p = 0.993$) showed that AChE fibers were lost throughout the auditory cortex after immunotoxin lesions of the NB. The cell loss, quantified by the number of p75 ^{NTR}-IR neurons, in the NB was always greater than the loss of cholinergic fibers in the cortex, as assessed by the density of AChE fibers. This is consistent with the finding that p75 ^{NTR} is a specific marker for cholinergic neurons in the basal forebrain (Tremere et al., 2000), whereas AChE histochemistry is not selective for cholinergic fibers but can also stain dopaminergic and other types of fibers (Mizukawa et al., 1986).

Importantly, the degree of cholinergic cell loss correlated positively with the sound localization impairments observed in animals that received ME20.4-SAP injections in the NB (Fig. 11, Table 2). Larger reductions of p75 ^{NTR}-IR cells in the NB produced greater impairments in localization performance. Modeling the degree of cholinergic cell loss against the

Table 1. Summary of histological analysis

	Corrected p75^{NTR} cell count ($n = 12$)		AChE fiber density (OF/μm^3) ($n = 6$)		
Experimental group	NB	Medial septum	PEG	MEG	AEG
Controls	1144 ± 253.6	3148 ± 730	0.840 ± 0.071	0.706 ± 0.067	0.669 ± 0.068
Cholinergic lesions	415 ± 432	2901 ± 477	0.761 ± 0.149	0.537 ± 0.177	0.568 ± 0.159

p75^{NTR}-IR neurons were quantified in serial sections through the NB and the medial septum for each hemisphere, and neuron counts were corrected for tissue volume using a method described by Konigsmark et al. (1969). AChE fiber density was quantified separately in the middle (MEG), anterior (AEG), and posterior (PEG) regions of the ectosylvian gyrus. Values are means ± SD. PV-IR neurons in the NB were quantified in the same way as p75^{NTR}-IR neurons (data not shown).

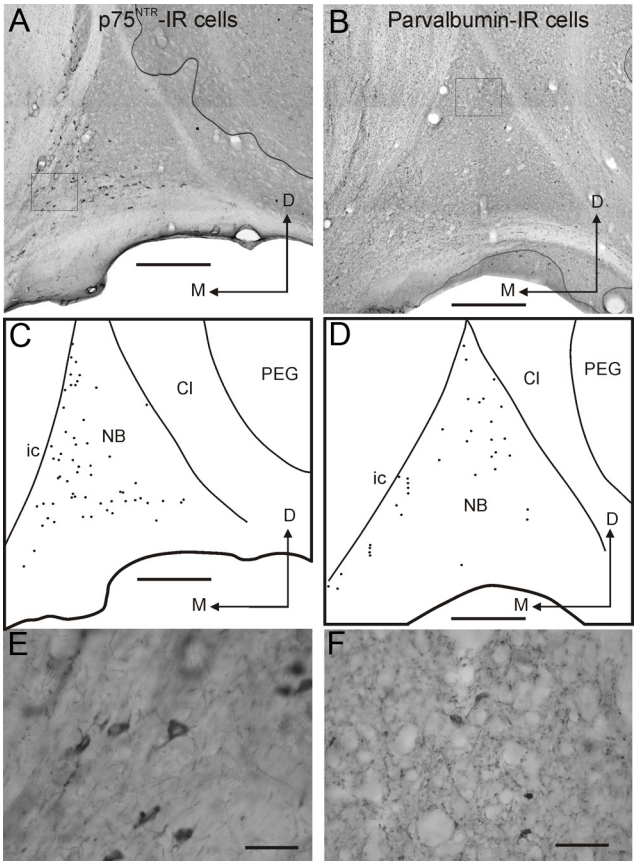

Figure 9. Distribution and morphology of neurons in the ferret NB that express p75^{NTR} (left column) or PV (right column). ***A***, ***B***, Pictures taken from coronal sections at the level of the NB in the right hemisphere showing the distribution of p75^{NTR} (***A***) and PV (***B***) IR neurons. ***C***, ***D***, Drawings of the same sections depicting the limits of the NB and the location of p75^{NTR} (***C***) and PV (***D***) IR neurons. ***E***, ***F***, Higher-magnification images of p75^{NTR} (***E***) and PV (***F***) positive neurons, with the squares in ***A*** and ***B*** representing the respective regions where these pictures were taken. CI, Claustrum; D, dorsal; ic, internal capsule; M, medial; PEG, posterior ectosylvian gyrus. Scale bars: ***A–D***, 0.5 mm; ***E***, ***F***, 50 μm.

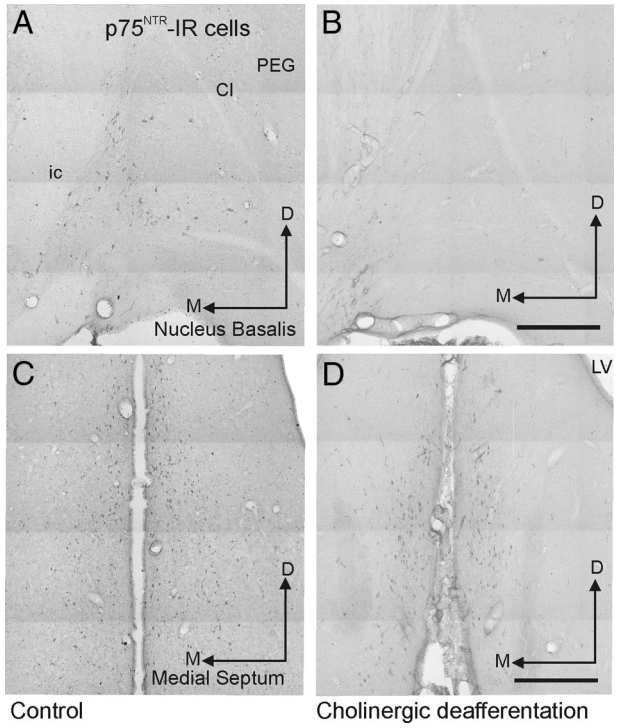

Figure 10. Bilateral ME20.4-SAP injections in the NB result in a local loss of p75^{NTR}-IR cells in that nucleus without affecting other cholinergic groups in the basal forebrain. These pictures were taken from coronal sections at the level of the NB (***A***, ***B***) and medial septum (***C***, ***D***). ***A*** and ***C*** are from a control animal, and ***B*** and ***D*** are from an animal in which ME20.4-SAP injections had been made in the NB. Scale bars, 0.5 mm. CI, Claustrum; ic, internal capsule; D, dorsal; M, medial; PEG, posterior ectosylvian gyrus.

proportion of correct responses revealed slopes significantly different from zero, particularly at the shortest stimulus durations (lme, 40–500 ms, $F_{(6,20)} = 9.02$, $p < 0.01$). There was also a significant effect of increasing cholinergic deafferentation on the mean error magnitude (lme, 40 ms, $F_{(1,6)} = 75.30$, $p < 0.01$) and the proportion of front–back errors (lme, 40 ms, $F_{(1,6)} = 37.54$, $p < 0.01$). Regression analysis of the proportion of correct responses versus cell loss (Fig. 11, Table 2) revealed a linear relationship between them with statistically significant negative slopes for stimulus durations of <1000 ms and increasing R^2 values as the duration was reduced (1000 ms, $R^2 = 0.194$, $p = 0.07$; 500 ms, $R^2 = 0.557$, $p = 0.03$; 200 ms, $R^2 = 0.512$, $p = 0.04$; 100 ms, $R^2 = 0.78$, $p = 0.003$; 40 ms, $R^2 = 0.88$, $p = 0.0005$). Therefore, these results reveal a strong correlation between loss of cortically projecting cholinergic neurons in the NB and the ability of ferrets to perform an approach-to-target localization task.

However, no clear relationship was found between the extent of cholinergic cell loss and adaptation in the earplugging experiments (Fig. 5, Table 2). Although the response gain at the end of the period of monaural occlusion was lowest in those animals in which a greater proportion of p75^{NTR}-IR cells in the NB had been lost, the slopes of the linear regressions fitted to the percentage correct scores versus training day did not show a consistent relationship with the degree of cholinergic deafferentation (Table 2). This suggests that relearning after monaural occlusion depends on the integrity of a minimum number of cholinergic cells in the NB. Thus, in contrast to the graded effects on sound localization accuracy found under normal hearing conditions, it appears that depletion of approximately one-third of the cholinergic neurons in the NB is sufficient to prevent spatial learning during a 9–10 d period of monaural occlusion.

In addition to including ACSF injections in the NB as part of our control group, we tested the specificity of ME20.4-SAP for cholinergic basal forebrain cells by injecting the immunotoxin in the caudate nucleus in one animal (Fig. 12). Both cholinergic (ChAT-IR) and GABAergic (PV-IR) neurons in the caudate ap-

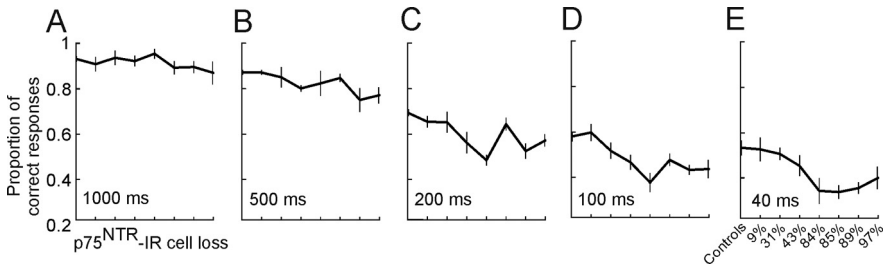

Figure 11. Effect of degree of cholinergic deafferentation on auditory localization performance. Proportion of correct responses (averaged over all loudspeaker locations) at five different stimulus durations for all animals with bilateral ME20.4-SAP immunotoxin injections in the NB, ordered by the percentage of loss of p75 ^{NTR}-IR neurons in the NB relative to control animals (see Table 2). Increasing cholinergic deafferentation led to progressively greater performance deficits, particularly at shorter stimulus durations. The degree of performance impairment positively correlated with the extent of cholinergic cell loss in the NB. Values plotted are means ± SD.

peared to be unaffected, even adjacent to the injection site (Fig. 12*A*, arrows), whereas the appearance and numbers of cholinergic neurons in the NB were similar to controls (Fig. 12*B*, arrows). In contrast to the deficits observed in ferrets with ME20.4-SAP injections in the NB (indicated in purple), the auditory localization performance of this animal closely resembled that of the controls (Fig. 12*C–E*), suggesting that the changes in behavior in the animals with NB injections are a specific consequence of the loss of cholinergic cells that express p75 ^{NTR}.

Discussion

Lesions (Jenkins and Masterton, 1982; Heffner and Heffner, 1990; Nodal et al., 2010) or reversible inactivation (Smith et al., 2004; Malhotra and Lomber, 2007) of the auditory cortex reduce sound localization accuracy, particularly for brief sounds. This is thought to reflect a deficit in both spatial discrimination and the ability to associate sounds with positions in space (Heffner and Heffner, 1990). Our results suggest that cholinergic neuromodulation of the neocortex influences the ability of ferrets to accurately perceive the locus of a sound source. Animals with cholinergic NB lesions exhibited global localization deficits, particularly at shorter stimulus durations, and were impaired in their ability to relearn to localize sound when challenged with a unilateral hearing impairment. Any changes in the cortical level of other neuromodulators that might have resulted from the selective loss of cholinergic neurons were not sufficient to rescue these behavioral deficits.

There is extensive evidence for cholinergic-dependent remodeling of auditory cortical receptive fields and sound frequency maps (Bakin and Weinberger, 1996; Kilgard and Merzenich, 1998a,b; Bao et al., 2003; Froemke et al., 2007), and this plasticity has been shown to influence auditory learning (Reed et al., 2011) and memory (Weinberger et al., 2006). Our results indicate that cholinergic modulation is required for both normal auditory processing and enabling animals to overcome perturbations in spatial cue composition with training. Reed et al. (2011) recently reported that pairing tones with NB stimulation facilitated the learning of a frequency discrimination task but had no effect on the discrimination abilities of rats that had previously learned the task. Although suggesting that cholinergic-dependent cortical plasticity does not influence performance on previously learned tasks, the detection of sensory cues that signify the presence of a reward has been shown to depend on the transient release of ACh in medial prefrontal cortex (mPFC) (Parikh et al., 2007).

We found that the ability of ferrets with cholinergic NB lesions to localize relatively brief sounds in an approach-to-target task was impaired without any corresponding effect on the accuracy of the initial head orienting responses. Because deactivating auditory cortex disrupts approach-to-target behavior but preserves head orienting accuracy (Nodal et al., 2012), this is consistent with a selective loss of cortical ACh. Moreover, the extent of this deficit in individual animals varied with the degree of cholinergic cell loss in the NB. In contrast, normal localization accuracy was observed if the stimulus duration was increased. However, this improvement in performance at longer stimulus durations was associated with longer response times, which potentially allowed the animals to benefit from additional spatial information resulting, for example, from movement of the head or increased integration time.

Therefore, animals with cholinergic lesions may have sacrificed response speed for improved performance when localizing these sounds, a performance strategy known as the speed–accuracy tradeoff (Fitts, 1954). This is consistent with a previous study showing that rats with cholinergic lesions of the basal forebrain are less able to detect visual stimuli in a serial reaction time task, an effect that disappears on increasing the duration of the stimulus (McGaughy et al., 2002). In monkeys, basal forebrain lesions disrupt spatial attention (Voytko et al., 1994), whereas depletion of ACh from prefrontal cortex impairs spatial working memory (Croxson et al., 2011). Rather than resulting from a change in neuronal spatial sensitivity in auditory cortex, the poorer ability of the ferrets with cholinergic lesions to localize shorter sounds could therefore reflect either an attentional deficit or greater difficulty in remembering from which speaker the stimulus had been presented under open-loop conditions in which the sound terminates before the head movement begins. It might be possible to distinguish between these possibilities by training animals to wait after stimulus presentation before initiating their response.

We also found that ferrets with cholinergic NB lesions were unable to relearn to localize sound after plugging one ear. Because cholinergic deafferentation resulted in less accurate approach-to-target behavior when short duration stimuli were used, the earplugging experiments were performed using longer stimuli (1000 ms), for which sound localization under normal hearing conditions was unaffected. Consequently, we can be confident that the lack of adaptation to an earplug represents a specific learning deficit. Pairing sounds with NB stimulation or direct ACh application can alter cortical sensitivity to multiple sound features (Weinberger, 2003). However, instead of shifting binaural cue sensitivity to compensate for the effects of the earplug, adaptation appears to involve learning to rely relatively more on the spectral cues available at the non-occluded ear and less on the cues that are altered by monaural occlusion (Kacelnik et al., 2006; Kumpik et al., 2010). ACh may influence this reweighting process by allowing shifts in sensitivity to these cues, thereby ensuring that appropriate combinations of inputs are integrated by auditory neurons. This is related to the notion that ACh release may modulate sensory processing, particularly under conditions of stimulus uncertainty (Yu and Dayan, 2005).

Alternatively, it may be the case that sustained attention is required to drive the adaptive changes that underlie such perceptual plasticity. St Peters et al. (2011) demonstrated that, when rats performing a visual detection task are challenged with distractor stimuli, the performance deficits observed correlate with increased ACh release in the mPFC. Although boosting cholinergic transmission by stimulating the nucleus accumbens substantially

Table 2. Relationship between cholinergic cell loss in the NB after bilateral ME20.4-SAP injections and behavioral performance in individual animals

Animal ID	% p75 ^{NTR}-IR cells lost in the NB			Sound localization accuracy (40 ms)	Response bias at end of monaural occlusion	Response gain at end of monaural occlusion	Regression slope during monaural occlusion (100×)
	Left	Right	Mean				
F0942 (×)	33%	30%	31.5%	49 ± 3%	0.078	0.685	1.7
F0940 (●)	75%	11%	43%	44 ± 5%	0.023	0.561	2.4
F0952 (◆)	83%	86%	84.5%	32 ± 6%	0.099	0.482	0.1
F0953	95%	77%	86%	32 ± 3%			
F0941 (▲)	84%	95%	89.5%	34 ± 3%	−0.212	0.354	1.3
F0954 (■)	97%	98%	97.5%	38 ± 5%	0.291	0.438	2.1
F0857	16%	2%	9%	51 ± 5%			

The percentage of p75 ^{NTR}-IR neurons lost in each hemisphere and the average loss are shown together with the percentage of correct responses (mean ± SD across all loudspeaker locations) on the sound localization task for 40 ms noise bursts, the response bias and gain in the relationship between stimulus and approach-to-target response location at the end of a 9–10 d period of monaural occlusion, and the slope of the linear regression of percentage correct score versus training day during this period. The monaural occlusion experiments were performed in five of these animals using 1000 ms noise bursts, as indicated by the symbols in the first column, which correspond to those used in Figure 5.

improves performance in the presence of a distractor, these improvements are attenuated by intracortical depletion of ACh. Together, these results suggest that increased cortical ACh release may be crucial for maintaining performance when perceptual tasks have to be performed under challenging circumstances, such as in the presence of distractor stimuli, when stimuli are particularly brief, or when sensory inputs are altered or become unreliable, as is the case for sound localization in the presence of a unilateral earplug. Therefore, this may account for the increased variability observed in the localization responses of animals with cholinergic lesions when one ear was occluded.

Our demonstration that the cholinergic system plays a critical role in training-dependent adaptive plasticity in the auditory system contrasts with the finding that the reorganization of the tonotopic map in the primary auditory cortex (A1) that takes place after the cochlea is partially lesioned is unaffected by injections of the same immunotoxin into the NB (Kamke et al., 2005b). However, a similar result has been described in the motor cortex. Thus, the basal forebrain cholinergic system is required for plasticity in adult animals when this is driven by skilled motor training but not by afferent nerve injury (Ramanathan et al., 2009). Consequently, a specific role for ACh in learning-induced plasticity that depends on behavioral experience appears to be a feature of both sensory and motor systems.

We found that cholinergic lesions of the NB resulted in a reduction in AChE fiber density in all the auditory cortical regions of the ferret. Therefore, we cannot exclude the possibility that cholinergic modulation in areas other than A1 might underlie the effects of cholinergic deafferentation on learning-induced plasticity of spatial hearing. In this regard, it is interesting to note that activity in higher-level auditory cortical areas, as well as A1, is required when ferrets learn to adapt to a unilateral earplug (Nodal et al., 2012).

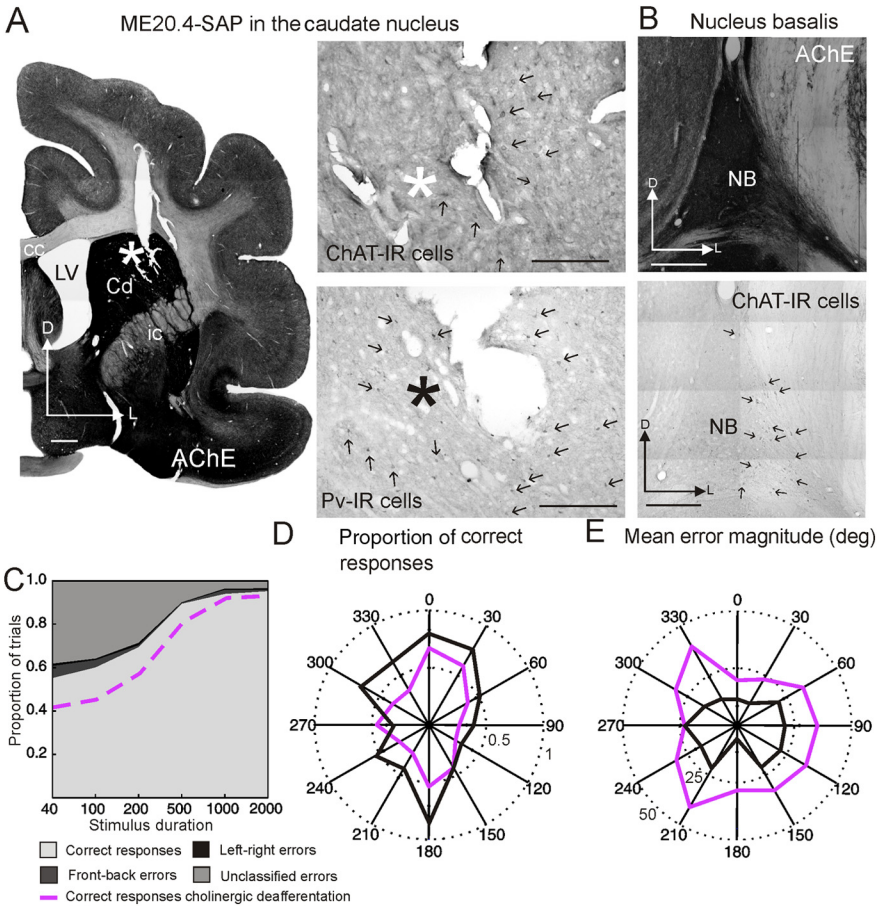

Figure 12. Sound localization performance did not change after ME20.4-SAP immunotoxin injections in the caudate nucleus (Cd). ***A***, Coronal section stained for AChE showing the ME20.4-SAP injection site in the Cd, plus higher magnification images of sections processed for ChAT and PV immunocytochemistry. Asterisks mark the end of the injection site, and arrows indicate immunopositive neurons. ***B***, Coronal sections at the level of the NB stained for AChE and ChAT; note the large number of ChAT-IR cells. ***C***, Approach-to-target localization responses at each stimulus duration. As in Figure 2, correct responses are shown in light gray, and incorrect responses are further subdivided into front–back errors (dark gray), left–right errors (black), and unclassified errors (mid-gray). The purple line indicates the mean percentage correct scores for the animals with cholinergic lesions of the NB. ***D***, ***E***, Polar plots illustrating the proportion of correct responses (***D***) and the mean error magnitude (***E***) at each peripheral speaker position when noise bursts with a duration of 40 ms were used. Data from the animals with ME20.4-SAP injections in the Cd and NB are shown in black and purple, respectively. Scale bars: ***A***, left, low-magnification image, 1 mm; ***A***, right, higher-magnification images, 0.5 mm; ***B***, 0.25 mm. cc, Corpus callosum; ic, internal capsule; D, dorsal; L, lateral; LV, lateral ventricle.

NB-induced receptive field plasticity in A1 (Miasnikov et al., 2001) and its associated memory (Miasnikov et al., 2008) depend on muscarinic receptors. However, ACh can also influence behavior via its effect on nicotinic receptors. For example, nicotine can improve accuracy and reduce response times in multiple-choice, visual stimulus detection tasks (Grilly et al. 2000; Hahn et al., 2002), which may be related to its facilitatory effect on

response gain in primary visual cortex (Disney et al., 2007; Bhattacharyya et al., 2012). Nicotinic receptor activation has also been implicated in regulating receptive field properties in A1 (Metherate, 2011). In particular, Liang et al. (2008) found that the effectiveness of nicotine in sharpening cortical frequency tuning is correlated with learning ability in adult rats. In addition, fear learning in mice requires cortex disinhibition that is mediated by nicotinic activation of layer I interneurons (Letzkus et al., 2011). Therefore, additional studies are required to determine which type of cholinergic receptor mediates the influence of the NB on auditory spatial processing and plasticity.

Our findings reveal the perceptual consequences for animals deprived of cortical cholinergic input, consequences that appear particularly marked when a task becomes harder, more complex, or requires greater attentional effort. The demonstration that the mature auditory system can compensate with training for an imbalance in inputs between the two ears has considerable implications for the capacity of patients to adapt to the altered sensory inputs associated, for example, with hearing aids or cochlear implants. The results of this study highlight the likely importance of cholinergic mechanisms of attention in adaptation under these conditions and suggest that neurodegenerative diseases associated with loss of forebrain cholinergic neurons will impair this learning process. Therefore, the role played by neuromodulatory systems will continue to be an important area for future research if we are to understand the complexities of how ongoing cognitive states of arousal and task engagement affect sensory processing.

References

Bajo VM, Nodal FR, Bizley JK, Moore DR, King AJ (2007) The ferret auditory cortex: descending projections to the inferior colliculus. Cereb Cortex 17:475–491. CrossRef Medline

Bajo VM, Nodal FR, Moore DR, King AJ (2010) The descending corticocollicular pathway mediates learning-induced auditory plasticity. Nat Neurosci 13:253–260. CrossRef Medline

Bakin JS, Weinberger NM (1996) Induction of a physiological memory in the cerebral cortex by stimulation of the nucleus basalis. Proc Natl Acad Sci U S A 93:11219–11224. CrossRef Medline

Bao S, Chang EF, Davis JD, Gobeske KT, Merzenich MM (2003) Progressive degradation and subsequent refinement of acoustic representations in the adult auditory cortex. J Neurosci 23:10765–10775. Medline

Bhattacharyya A, Bießmann F, Veit J, Kretz R, Rainer G (2012) Functional and laminar dissociations between muscarinic and nicotinic cholinergic neuromodulation in the tree shrew primary visual cortex. Eur J Neurosci 35:1270–1280. CrossRef Medline

Cordery PM, Bajo VM, Leach ND, King AJ (2009) The cholinergic basal forebrain in the ferret and its inputs to the auditory cortex. Assoc Res Otolaryngol Abs 136.

Croxson PL, Kyriazis DA, Baxter MG (2011) Cholinergic modulation of a specific memory function of prefrontal cortex. Nat Neurosci 14:1510–1512. CrossRef Medline

Disney AA, Aoki C, Hawken MJ (2007) Gain modulation by nicotine in macaque V1. Neuron 56:701–713. CrossRef Medline

Edeline JM (2012) Beyond traditional approaches to understanding the functional role of neuromodulators in sensory cortices. Front Behav Neurosci 6:45. CrossRef Medline

Fitts PM (1954) The information capacity of the human motor system in controlling the amplitude of movement. J Exp Psychol 47:381–391. CrossRef Medline

Froemke RC, Merzenich MM, Schreiner CE (2007) A synaptic memory trace for cortical receptive field plasticity. Nature 450:425–429. CrossRef Medline

Gallyas F (1979) Silver staining of myelin by means of physical development. Neurol Res 1:203–209. Medline

Goard M, Dan Y (2009) Basal forebrain activation enhances cortical coding of natural scenes. Nat Neurosci 12:1444–1449. CrossRef Medline

Grilly DM, Simon BB, Levin ED (2000) Nicotine enhances stimulus detection performance of middle- and old-aged rats: a longitudinal study. Pharmacol Biochem Behav 65:665–670. CrossRef Medline

Gritti I, Manns ID, Mainville L, Jones BE (2003) Parvalbumin, calbindin, or calretinin in cortically projecting and GABAergic, cholinergic, or glutamatergic basal forebrain neurons of the rat. J Comp Neurol 458:11–31. CrossRef Medline

Gundersen HJ, Bagger P, Bendtsen TF, Evans SM, Korbo L, Marcussen N, Møller A, Nielsen K, Nyengaard JR, Pakkenberg B, Sørensen FB, Vesterby A, West MJ (1988) The new stereological tools: disector, fractionator, nucleator and point sampled intercepts and their use in pathological research and diagnosis. APMIS 96:857–881. CrossRef Medline

Hahn B, Shoaib M, Stolerman IP (2002) Nicotine-induced enhancement of attention in the five-choice serial reaction time task: the influence of task demands. Psychopharmacology (Berl) 162:129–137. CrossRef Medline

Hasselmo ME, Sarter M (2011) Modes and models of forebrain cholinergic neuromodulation of cognition. Neuropsychopharmacology 36:52–73. CrossRef Medline

Heffner HE, Heffner RS (1990) Effect of bilateral auditory cortex lesions on sound localization in Japanese macaques. J Neurophysiol 64:915–931. Medline

Herrero JL, Roberts MJ, Delicato LS, Gieselmann MA, Dayan P, Thiele A (2008) Acetylcholine contributes through muscarinic receptors to attentional modulation in V1. Nature 454:1110–1114. CrossRef Medline

Jenkins WM, Masterton RB (1982) Sound localization: effects of unilateral lesions in central auditory system. J Neurophysiol 47:987–1016. Medline

Kacelnik O, Nodal FR, Parsons CH, King AJ (2006) Training-induced plasticity of auditory localization in adult mammals. PLoS Biol 4:627–638. CrossRef Medline

Kamke MR, Brown M, Irvine DR (2005a) Origin and immunolesioning of cholinergic basal forebrain innervation of cat primary auditory cortex. Hear Res 206:89–106. CrossRef Medline

Kamke MR, Brown M, Irvine DRF (2005b) Basal forebrain cholinergic input is not essential for lesion-induced plasticity in mature auditory cortex. Neuron 48:675–686. CrossRef Medline

Kilgard MP, Merzenich MM (1998a) Cortical map reorganization enabled by nucleus basalis activity. Science 279:1714–1718. CrossRef Medline

Kilgard MP, Merzenich MM (1998b) Plasticity of temporal information processing in the primary auditory cortex. Nat Neurosci 1:727–731. CrossRef Medline

Klinkenberg I, Sambeth A, Blokland A (2011) Acetylcholine and attention. Behav Brain Res 221:430–442. CrossRef Medline

Konigsmark BW, Kalyanaraman UP, Corey P, Murphy EA (1969) An evaluation of techniques in neuronal population estimates: the sixth nerve nucleus. Johns Hopkins Med J 125:146–158. Medline

Kordower JH, Gash DM, Bothwell M, Hersh L, Mufson EJ (1989) Nerve growth factor receptor and choline acetyltransferase remain colocalized in the nucleus basalis (Ch4) of Alzheimer's patients. Neurobiol Aging 10:67–74. CrossRef Medline

Kumpik DP, Kacelnik O, King AJ (2010) Adaptive reweighting of auditory localization cues in response to chronic unilateral earplugging in humans. J Neurosci 30:4883–4894. CrossRef Medline

Lacouture Y, Cousineau D (2008) How to use MATLAB to fit the ex-Gaussian and other probability functions to a distribution of response times. Tutor Quant Methods Psychol 4:35–45.

Lehmann J, Nagy JI, Atmadia S, Fibiger HC (1980) The nucleus basalis magnocellularis: the origin of a cholinergic projection to the neocortex of the rat. Neuroscience 5:1161–1174. CrossRef Medline

Letzkus JJ, Wolff SB, Meyer EM, Tovote P, Courtin J, Herry C, Lüthi A (2011) A disinhibitory microcircuit for associative fear learning in the auditory cortex. Nature 480:331–335. CrossRef Medline

Liang K, Poytress BS, Weinberger NM, Metherate R (2008) Nicotinic modulation of tone-evoked responses in auditory cortex reflects the strength of prior auditory learning. Neurobiol Learn Mem 90:138–146. CrossRef Medline

Ma X, Suga N (2003) Augmentation of plasticity of the central auditory system by the basal forebrain and/or somatosensory cortex. J Neurophysiol 89:90–103. Medline

Malhotra S, Lomber SG (2007) Sound localization during homotopic and heterotopic bilateral cooling deactivation of primary and nonprimary auditory cortical areas in the cat. J Neurophysiol 97:26–43. CrossRef Medline

McGaughy J, Dalley JW, Morrison CH, Everitt BJ, Robbins TW (2002) Se-

lective behavioral and neurochemical effects of cholinergic lesions produced by intrabasalis infusions of 192 IgG-saporin on attentional performance in a five-choice serial reaction time task. J Neurosci 22:1905–1913. Medline

Mesulam MM, Mufson EJ, Levey AI, Wainer BH (1983) Cholinergic innervation of cortex by the basal forebrain: cytochemistry and cortical connections of the septal area, diagonal band nuclei, nucleus basalis (substantia innominata), and hypothalamus in the rhesus monkey. J Comp Neurol 214:170–197. CrossRef Medline

Metherate R (2011) Functional connectivity and cholinergic modulation in auditory cortex. Neurosci Biobehav Rev 35:2058–2063. CrossRef Medline

Metherate R, Cox CL, Ashe JH (1992) Cellular bases of neocortical activation: modulation of neural oscillations by the nucleus basalis and endogenous acetylcholine. J Neurosci 12:4701–4711. Medline

Miasnikov AA, McLin D 3rd, Weinberger NM (2001) Muscarinic dependence of nucleus basalis induced conditioned receptive field plasticity. Neuroreport 12:1537–1542. CrossRef Medline

Miasnikov AA, Chen JC, Weinberger NM (2008) Specific auditory memory induced by nucleus basalis stimulation depends on intrinsic acetylcholine. Neurobiol Learn Mem 90:443–454. CrossRef Medline

Mizukawa K, McGeer PL, Tago H, Peng JH, McGeer EG, Kimura H (1986) The cholinergic system of the human hindbrain studied by choline acetyltransferase and acetylcholinesterase histochemistry. Brain Res 379:39–55. CrossRef Medline

Nodal FR, Bajo VM, Parsons CH, Schnupp JW, King AJ (2008) Sound localization behavior in ferrets: comparison of acoustic orientation and approach-to-target responses. Neuroscience 154:397–408. CrossRef Medline

Nodal FR, Kacelnik O, Bajo VM, Bizley JK, Moore DR, King AJ (2010) Lesions of the auditory cortex impair azimuthal sound localization and its recalibration in ferrets. J Neurophysiol 103:1209–1225. CrossRef Medline

Nodal FR, Bajo VM, King AJ (2012) Plasticity of spatial hearing: behavioural effects of cortical inactivation. J Physiol 590:3965–3986. CrossRef Medline

Oldford E, Castro-Alamancos MA (2003) Input-specific effects of acetylcholine on sensory and intracortical evoked responses in the "barrel cortex" in vivo. Neuroscience 117:769–778. CrossRef Medline

Panzeri S, Senatore R, Montemurro MA, Petersen RS (2007) Correcting for the sampling bias problem in spike train information measures. J Neurophysiol 98:1064–1072. CrossRef Medline

Parikh V, Kozak R, Martinez V, Sarter M (2007) Prefrontal acetylcholine release controls cue detection on multiple timescales. Neuron 56:141–154. CrossRef Medline

Pizzo DP, Waite JJ, Thal LJ, Winkler J (1999) Intraparenchymal infusions of 192 IgG-saporin: development of a method for selective and discrete lesioning of cholinergic basal forebrain nuclei. J Neurosci Methods 91:9–19. CrossRef Medline

Ramanathan D, Tuszynski MH, Conner JM (2009) The basal forebrain cholinergic system is required specifically for behaviorally mediated cortical map plasticity. J Neurosci 29:5992–6000. CrossRef Medline

Reed A, Riley J, Carraway R, Carrasco A, Perez C, Jakkamsetti V, Kilgard MP (2011) Cortical map plasticity improves learning but is not necessary for improved performance. Neuron 70:121–131. CrossRef Medline

Schnupp J, Nelken I, King A (2010) Auditory neuroscience: making sense of sound. Cambridge, MA: Massachusetts Institute of Technology.

Sillito AM, Kemp JA (1983) Cholinergic modulation of the functional organization of the cat visual cortex. Brain Res 289:143–155. CrossRef Medline

Smith AL, Parsons CH, Lanyon RG, Bizley JK, Akerman CJ, Baker GE, Dempster AC, Thompson ID, King AJ (2004) An investigation of the role of auditory cortex in sound localization using muscimol-releasing Elvax. Eur J Neurosci 19:3059–3072. CrossRef Medline

St Peters M, Demeter E, Lustig C, Bruno JP, Sarter M (2011) Enhanced control of attention by stimulating mesolimbic-corticopetal cholinergic circuitry. J Neurosci 31:9760–9771. CrossRef Medline

Tago H, Kimura H, Maeda T (1986) Visualization of detailed acetylcholinesterase fiber and neuron staining in rat brain by a sensitive histochemical procedure. J Histochem Cytochem 34:1431–1438. CrossRef Medline

Tremere LA, Pinaud R, Grosche J, Härtig W, Rasmusson DD (2000) Antibody for human p75 LNTR identifies cholinergic basal forebrain of nonprimate species. Neuroreport 11:2177–2183. CrossRef Medline

Voytko ML, Olton DS, Richardson RT, Gorman LK, Tobin JR, Price DL (1994) Basal forebrain lesions in monkeys disrupt attention but not learning and memory. J Neurosci 14:167–186. Medline

Weinberger NM (2003) The nucleus basalis and memory codes: auditory cortical plasticity and the induction of specific, associative behavioral memory. Neurobiol Learn Mem 80:268–284. CrossRef Medline

Weinberger NM, Miasnikov AA, Chen JC (2006) The level of cholinergic nucleus basalis activation controls the specificity of auditory associative memory. Neurobiol Learn Mem 86:270–285. CrossRef Medline

Yu AJ, Dayan P (2005) Uncertainty, neuromodulation, and attention. Neuron 46:681–692. CrossRef Medline

Zhang Y, Yan J (2008) Corticothalamic feedback for sound-specific plasticity of auditory thalamic neurons elicited by tones paired with basal forebrain stimulation. Cereb Cortex 18:1521–1528. CrossRef Medline